



## Contribution of Methyl Substituent on the Conductivity Properties and Behaviour of CMC-Alkoxy Thiourea Polymer Electrolyte

Saidatul Radhiah Ghazali, K. Kubulat, M. I. N. Isa, A. S. Samsudin & Wan M. Khairul

**To cite this article:** Saidatul Radhiah Ghazali, K. Kubulat, M. I. N. Isa, A. S. Samsudin & Wan M. Khairul (2014) Contribution of Methyl Substituent on the Conductivity Properties and Behaviour of CMC-Alkoxy Thiourea Polymer Electrolyte, *Molecular Crystals and Liquid Crystals*, 604:1, 126-141, DOI: [10.1080/15421406.2014.968058](https://doi.org/10.1080/15421406.2014.968058)

**To link to this article:** <http://dx.doi.org/10.1080/15421406.2014.968058>



Published online: 15 Dec 2014.



Submit your article to this journal [↗](#)



Article views: 21



View related articles [↗](#)



View Crossmark data [↗](#)

# Contribution of Methyl Substituent on the Conductivity Properties and Behaviour of CMC-Alkoxy Thiourea Polymer Electrolyte

SAIDATUL RADHIAH GHAZALI, K. KUBULAT,  
M. I. N. ISA, A. S. SAMSUDIN, AND WAN M. KHAIRUL\*

School of Fundamental Science, Universiti Malaysia Terengganu,  
Terengganu, Malaysia

*An essentially linear conjugated thiourea system provides wide range of electronic properties as they consist of rigid  $\pi$ -systems on their structures. This study reported the synthetic, characterization and theoretical evaluation of molecular wire candidate bearing alkoxy thiourea derivative featuring methylbenzene head group. It was applied as dopant in Carboxymethyl-Cellulose (CMC) solution in order to form a conductive biodegradable thin film. According to the conductivity result, the developed system can be developed as electrical conductor as proven via both experimental and theoretical studies. Therefore, this type of A-ArC(O)NHC(S)NHAr-D molecular framework has opened wide possibilities to be applied in many micro-electronic application devices.*

**Keywords** Thiourea; carboxymethyl-cellulose (CMC); polymer electrolyte; Gaussian

## 1. Introduction

Throughout many years, thiourea derivatives have been applied widely in numerous fields such as in agricultural [1], pharmaceutical [2], and also in sensory application [3]. As described in literature, the unique properties of thiourea make it becomes versatile compound to be applied in those fields. The presence of diprotic donor groups of thiourea compound make it becomes good receptors for anion detection [4]. Moreover, it has a high crystallographic symmetry to make it behaves as a good ligand in complexes [5]. In addition, the exploitation of thiourea molecular backbone by introducing  $\pi$ -system makes it as a good candidate as molecular wires by making use of the electronic properties which can be generated in situ at the molecular framework potentially for numerous potential applications [6–8].

To date, the development of molecular wires in the conjugated polymer has become a great attention in order to design high capable molecular system [9]. There is an urge to find the ideal materials in the form of membrane applied in microelectronic devices. To the best of our knowledge, there is no work has been carried out on thiourea moieties to fulfil

---

\*Address correspondence to Wan M. Khairul, School of Fundamental Science, Universiti Malaysia Terengganu, 21030 Kuala Terengganu, Terengganu, Malaysia. E-mail: wmkhairul@umt.edu.my

Color versions of one or more of the figures in the article can be found online at [www.tandfonline.com/gmcl](http://www.tandfonline.com/gmcl).

this current demand. Based on literatures, the study on conductive membrane has become a phenomenon for researchers' interest to discover an ideal polymer host in electrolytes system. The use of cellulose as a polymer host in electrolytes system has been reported to afford good mechanical properties and ease to handle [10].

One of the most well-known cellulose derivatives is Carboxymethyl Cellulose (CMC). It is also known as cellulose gum. CMC is an anionic, water-soluble cellulose ether and available in a wide range of substitution. CMC is an abundant and naturally occurring polymer exhibiting good mechanical properties, renewable and biodegradable [11–12]. However, the use of CMC itself as a polymer host has achieved moderate results of conductivity [13]. To overcome this problem, the use of suitable dopant in the polymer host system is needed in order to increase the conductivity.

It is a great challenge for a researcher to find a compound that can be an ideal dopant for CMC polymer. The characteristic of dopant must be suitable with the CMC properties in chemical and mechanical aspects. As a versatile compound with the rigid  $\pi$ -system on its structures, thiourea has a large potential to be a candidate as a dopant for CMC polymer host. Thus, the aims of this study are to design, prepare and characterize novel thiourea-based conjugated compounds prior to the formation of a solid conductive membrane. The important of thiourea derivatives in this study is to act as a dopant in order to increase the conductivity of CMC.

## 2. Experimental

### 2.1 Materials and General Methodology

All chemicals or reagents used in this study were purchased from standard commercial suppliers and used as received without further purification. The infrared (IR) spectra were recorded on a Fourier Transform-Infrared Spectrometer, Perkin Elmer Spectrum 100 in the range of 4000–400  $\text{cm}^{-1}$  using potassium bromide (KBr) pellets. Electronic absorption spectra of the samples were recorded in 1 cm path length quartz cell within range of 200–400 nm using Shimadzu UV-Vis Spectrophotometer 1601 series and Carry Varian 200 concentration. The NMR spectra were recorded on Bruker Avance 300 ( $^1\text{H}$  400.11 MHz,  $^{13}\text{C}$  100.61 MHz) spectrometer from deuterated  $\text{CDCl}_3$  solution at room temperature as solvent and internal standard in the range between  $\delta_{\text{H}}$  0–15 ppm ( $^1\text{H}$ ) and  $\delta_{\text{C}}$  0–200 ppm ( $^{13}\text{C}$ ). The solvent and chemical shift values were given in parts per million (ppm) relative to solvent resonance as internal standard. The C, H, N and S microanalysis was carried out with FLASH EA 1112 CHNS-O analyzer. The Thermogravimetric analysis was performed using Perkin-Elmer TGA Analyzer from 0°C to 700°C at a heating rate of 10°C/min under nitrogen atmosphere. Analytical thin-layer chromatography (TLC) was carried out on precoated plate of TLC Silica Gel 60 F<sub>254</sub> (Merck), and spots were visualized with ultraviolet light. While the XRD patterns were recorded at room temperature on a MiniFlex II diffraction equipped with an X'celerator, using Cu K $\alpha$  radiation in the range of  $2\theta = 5^\circ - 80^\circ$ . The experimental results were proven by using Gaussian 09 quantum mechanical software package at the theoretical level of DFT (B3LYP)/6-31G (d,p). The required physical parameters such as dipole moment, energy band gap (HOMO and LUMO), molar volume, molecular radii, Wiberg bond index, bond length and NBO charges were evaluated using Natural Bond Orbital Theory at the same theoretical level as for optimization. Electrical conductivity characterization was determined using HIOKI

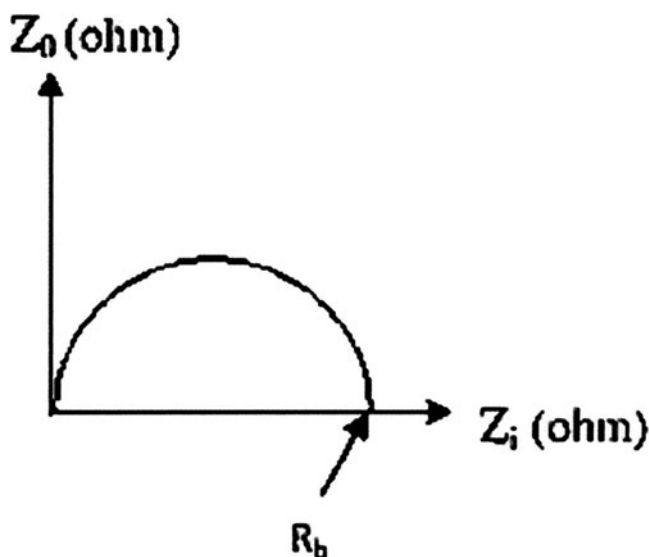


Figure 1. Cole-Cole Plot.

3531 High-Tester Electrical Impedance Spectroscopy (EIS) in frequency range 50 Hz-1 MHz.

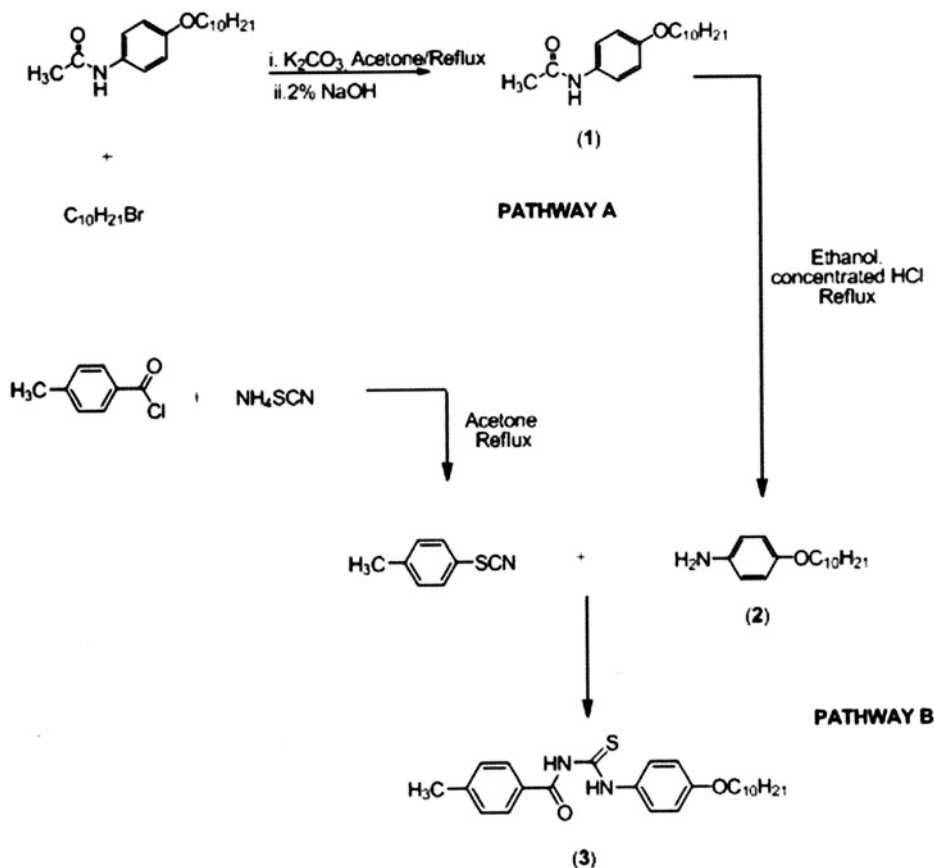
The biodegradable film, **4** was prepared by the solution casting technique. 1 g carboxymethyl cellulose (Acros Organic Co.) was dissolved in 50 ml of water whilst in another different beaker, 0.5 g of **3** was dissolved in 50 ml methanol with constant stirring at 30°C - 40°C respectively. The solution of **3a** was added into CMC solution while stirring to form homogenous dissolution. The mixture was then poured into several Petri dishes and allowed to evaporate slowly at ambient temperature for film to form. The bulk resistant ( $R_b$ ) value was obtained from the plot of negative imaginary impedance versus real part of impedance versus real part of impedance and the conductivity ( $\sigma$ ) of the sample was calculated from Equation (1):

$$\sigma = \frac{t}{R_b a} \quad (1)$$

since,  $t$  = thickness of film,  $a$  = area of film and  $R_b$  = bulk resistant

The plot of negative imaginary impedance versus real part of impedance gives the Cole-Cole Plot as shown in Fig. 1. This plot is very useful since it was used to calculate the ionic conductivity of the sample using the Equation (1).

The synthesis of *N*-decyloxyphenyl-*N'*-(methylbenzoyl) thiourea (**3**) derivative involved several continuous reaction which were *N*-(4-(decyloxy)phenyl) acetamide (**1**) as precursor, and 4-decyloxy aniline (**2**) as intermediate. For **1** and **2**, the synthetic work and analytical characterisation have been reported in previous occasions [14–15]. The synthetic pathway in the preparation of the final product of interest, (**3**) is described in Scheme 1 which involves two continuous synthetic pathways, namely A and B.



**Scheme 1.** Synthesis of N-dexyloxyphenyl-N'-(methylbenzoyl) thiourea (3).

## 2.2 Experimental

**2.2.1 Preparation of N-(octyloxy)phenyl-N'-(benzene-1,3-dicarbonyl) thiourea (3).** A suspension of 4-methyl benzoyl chloride (5.8 g, 37.8 mmol) in 50 ml acetone was added into ammonium thiocyanate (2.9 g, 37.8 mmol) in 50 ml acetone to give off-white solution. The solution was stirred at room temperature for 4 hours, followed by addition of 4-decyloxy aniline (9.4 g, 37.8 mmol). After stirring for another 1 hour, the colour of the solution turned from off-white to white. After adjudged completion by thin layer chromatography (hexane: dichloromethane) (2:3 ratio), the reaction mixture was cooled to room temperature and filtered. The off-white filtrate was added with 3-5 ice cubes and filtered to obtain white precipitate. The white precipitate was then recrystallized from methanol to afford the white crystalline solid of the title compound, **3** (4.5 g, 10 mmol, 65%). IR  $\nu$ (N-H) 3307,  $\nu$ (C = O) 1673,  $\nu$ (C = S) 830  $cm^{-1}$ .  $^1H$  NMR:  $\delta$  0.91 (t,  $J_{HH} = 7$  Hz, 3H,  $CH_3$ ), 1.30–1.84 (m, 16H, 8 x  $CH_2$ ), 2.47 (s, 3H,  $CH_3$ ), 3.98 (t,  $J_{HH} = 6$  Hz, 2H,  $CH_2$ ), 6.96 (pseudo-d,  $J_{HH} = 9$  Hz, 2H,  $C_6H_4$ ), 7.37 (pseudo-d,  $J_{HH} = 8$  Hz, 2H,  $C_6H_4$ ), 7.58 (pseudo-d,  $J_{HH} = 9$  Hz, 2H,  $C_6H_4$ ), 7.82 (pseudo-d,  $J_{HH} = 8$  Hz, 2H,  $C_6H_4$ ), 9.12, 12.47 (2 x s, 1H, NH).  $^{13}C$  {H} NMR:  $\delta$  14.14, 21.70 ( $CH_3$ ), 21.70–31.91 (8 x  $CH_2$ ), 68.26 ( $CH_2$ -O), 128.80 - 157.88 (s, CH), 114.63, 125.79, 128.90, 130.38 ( $C_6H_4$ ), 166.87 (s, C = O), 178.71 (s, C = S). Found:

**Table 1.** The main electronic absorption data of **1**, **2** and **3**

| Compounds | $\lambda$ (nm) (absorbance, extinction coefficient, $\varepsilon$ ( $\text{M}^{-1} \text{cm}^{-1}$ )) |                         |                            |                            |  |
|-----------|---|-------------------------|----------------------------|----------------------------|--|
|           | Band 1  | Assignment              | Band 2                     | Band 3                     | Assignment   |
| <b>1</b>  | 251.1 (0.541,<br>76607.0)   | $\pi \rightarrow \pi^*$ | 278.8 (0.0543,<br>6368.0)  | —                          | $\pi \rightarrow \pi^*$                                |
| <b>2</b>  | 225.2 (0.658,<br>83416.0)   | $\pi \rightarrow \pi^*$ | 276.0 (0.1001,<br>10323.0) | 283.0 (0.0845,<br>9472.0)  | $\pi \rightarrow \pi^*$                                |
| <b>3</b>  | 238.0 (0.583,<br>80217.0)   | $\pi \rightarrow \pi^*$ | 276.2 (0.0622,<br>8684.0)  | 281.2 (0.1241,<br>12973.0) | Mixed $n \rightarrow \pi^*$<br>$\pi \rightarrow \pi^*$ |

C, 70.37; H, 7.29; N, 6.29; S, 7.53%.  $\text{C}_{25}\text{H}_{34}\text{N}_2\text{O}_2\text{S}$  requires: C, 70.22; H, 7.67; N, 6.55; S, 6.86%.

### 3. Results and Discussion

#### 3.1 UV-Visible Analysis of **1**, **2** and **3**

All synthesized compounds (**1**, **2** and **3**) contain aromatic systems which is responsible for  $\pi \rightarrow \pi^*$  transition which typically contributed by primary and secondary bands phenyl rings.

The distinctive bands of these compounds were observed at around 201–210 nm ( $\xi = 9178$  to  $117375 \text{ M}^{-1}$ ) and 220–270 nm ( $\xi = 9178$  to  $1121995 \text{ M}^{-1}$ ) which can be assigned as  $\pi \rightarrow \pi^*$  transition. Recent evidence suggests that the absorptions shifted strongly to  $\pi \rightarrow \pi^*$  transition at lower wavelengths and molar absorptivity influenced by the inductive effect interaction between the phenyl ring and carbonyl groups [16–18]. Additionally, substitution on phenyl ring by auxochrome namely  $-\text{NH}$  and  $-\text{CH}_3$ , substituents groups in these synthesized compounds can cause bathochromic and hyperchromic shifts in the spectra. However, it can be seen that the secondary bands contributed by phenyl rings were overlapped with carbonyl groups. Whilst, the transition for the primary and secondary bands also appeared strongly perturbing by the chromophores of methanol solvent which arise *ca.* 201–230 nm (Fig. 2) (Table 1).

The band occurs in the region from 220–270 nm ( $\xi = 9178$  to  $1121995 \text{ M}^{-1} \text{cm}^{-1}$ ) resulting from the  $n \rightarrow \pi^*$  and  $\pi \rightarrow \pi^*$  transitions could be due to the lone pair of electrons on the oxygen of  $\text{C}=\text{O}$ . These transition shifts to longer wavelength are attributed to the conjugation between of carbonyl groups participate in resonance with the rings which is presumably due to  $n \rightarrow \pi^*$  transition of the carbonyl group and  $\pi \rightarrow \pi^*$  transition of the carbonyl group and the aromatic ring.

On the other hand, the presence of auxochromes  $-\text{NH}$  as electron donating attached to carbonyl and thione in these compounds which leads to the bathochromic shifts on the  $n \rightarrow \pi^*$  and  $\pi \rightarrow \pi^*$  transitions at *ca.* 220–238 nm. These characteristics are might be due to the inductive effect of nitrogen which withdraws electrons from the carbonyl and thione carbon using the lone pair electrons on the oxygen and sulphur atom to be more held tightly through bound electrons between each other. Three bands in these compounds are also affected by the polarity of the solvents increase in the  $n \rightarrow \pi^*$  and  $\pi \rightarrow \pi^*$  transitions undergo bathochromic shift [16–17, 19]. These transition shifts to longer wavelength or

**Table 2.** Result for three types of energy band gaps between different transitions for **3**

| $\Delta\xi_A$ of the max population to the max population, eV | $\Delta\xi_B$ of the largest transition, eV | $\Delta\xi_C$ of the lowest transition, eV |
|---|---|--|
| 4.49 ( $\lambda_{\max} = 276$ nm)                             | 4.86 ( $\lambda_{\text{upp}} = 255$ nm)     | 4.04 ( $\lambda_{\text{low}} = 307$ nm)    |
| 4.43 ( $\lambda_{\max} = 280$ nm)                             | 4.79 ( $\lambda_{\text{upp}} = 259$ nm)     | 3.76 ( $\lambda_{\text{low}} = 376$ nm)    |

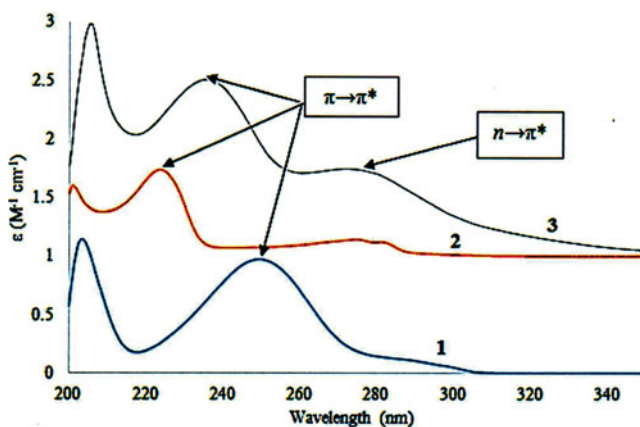
lower energy in polar solvent because the transitions have polar excited state which was stabilized by hydrogen bonding.

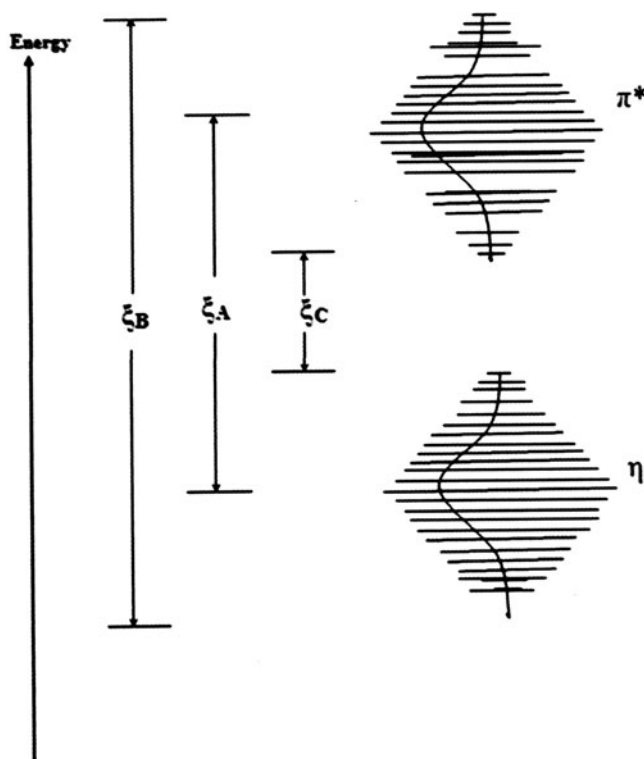
All these compounds give rise to three absorption bands which were assigned as a mixture of  $n \rightarrow \pi^*$  and  $\pi \rightarrow \pi^*$  transitions. The methyl substituent on phenyl ring, the presence of auxochromes  $-\text{NH}$  interaction at chromospheres  $\text{C}=\text{O}$  and  $\text{C}=\text{S}$ , and solvent effect may generate a bathochromic effect in these spectra. Furthermore, the energy band gap also can be calculated using these UV spectra. For these system of thiourea molecules the energy band gap is just the different between the non-bonding ' $n$ ' molecular orbital and the anti-bonding of ' $\pi^*$ ' molecular orbital or in other word between the HOMO and LUMO of the system. For a clear view, the types of energy band gaps for  $n \rightarrow \pi^*$  transition sketch according to their molecular orbital energy level is illustrated in Scheme 2. The energy of the  $n \rightarrow \pi^*$  transition is therefore between  $\Delta\xi_B$  and  $\Delta\xi_C$ , where the maximum transition is at  $\Delta\xi_A$ .

In order to ease the understanding of the energy band gap of the system, in Table 2 depicts the results of three types of energy band gaps between the maximum population ( $\Delta\xi_A$ ), the maximum energy transition ( $\Delta\xi_B$ ) and the minimum energy transition ( $\Delta\xi_C$ ).

### 3.2 Characterization of CMC-thiourea Polymer Electrolyte, **4**

In order to determine the complexation between CMC and thiourea compound (**3**), the CMC-thiourea thin film was characterized via FT-IR and X-Ray Diffraction Spectroscopy. In addition, Electrical Impedance Spectroscopy study was done in order to measure

**Figure 2.** UV-Vis spectra for **1**, **2** and **3**.



**Scheme 2.** Types of energy band gaps for  $n \rightarrow \pi^*$  transition sketch according to their molecular orbital energy levels.

the conductivity of the polymer electrolyte. Furthermore, to support the experimental results obtained, Gaussian 09 Software was used in order to provide the theoretical data of the physical parameter. The composition of the CMC-thiourea polymer electrolyte is abbreviated as **4** with film thickness was 0.014 cm.

**3.2.1 Fourier Transform Infrared (FTIR) Spectroscopy Analysis.** FTIR analysis was carried out to determine the complexation between CMC and thiourea, **3** and to prove the conductivity species in the CMC-thiourea system. In this task, carboxymethyl cellulose (CMC) was used as the host whereas **3** was used as the dopant material. Fig. 3 depicts the spectrum of pure CMC powders in the region from 700 to 3700  $\text{cm}^{-1}$ .

For pure CMC spectrum, a very strong absorbance band at 3439  $\text{cm}^{-1}$  was observed and can be assigned to the vibrations of the intra-molecular hydrogen bond ( $\nu_{\text{OH}}$ ). The peak at 2920  $\text{cm}^{-1}$  and 1377  $\text{cm}^{-1}$  were assigned to stretching and bending vibrations of the C-H bond ( $\nu_{\text{CH}}$  and  $\delta_{\text{CH}}$  respectively). The strong peak at 1605  $\text{cm}^{-1}$  was the stretching vibrations in the carboxylic group ( $\nu_{\text{COOH}}$ ). Additionally, a strong peak at 1072  $\text{cm}^{-1}$  was assigned to bending vibrations of the ether (glycosidic) linkage ( $\delta_{\text{C-O-C}}$ ).

In order to determine and study the complexation between CMC and thiourea, the FTIR spectrum of thiourea, **3** was compared with FTIR spectrum of CMC-thiourea polymer electrolyte, (**4**) (Fig. 4).

From the spectra above clearly, there are slightly different at the intensity of peaks of thiourea dopant (**3**) with the addition of CMC. In system **4** spectrum, the intensity of



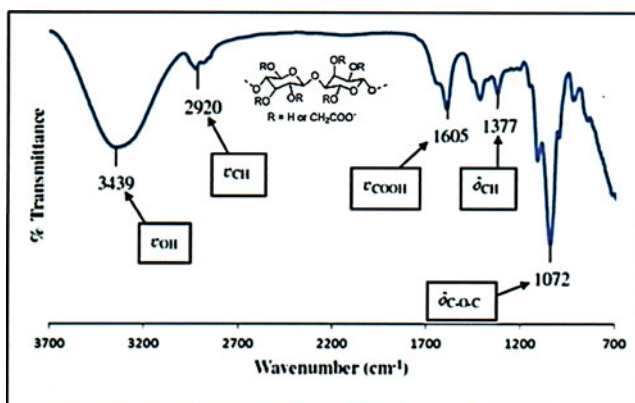


Figure 3. FTIR spectrum of pure CMC.

most peaks which represent the main functional groups of thiourea decreases due to the interaction of thiourea compounds with the CMC to form a new polymer electrolytes thin films. Furthermore, in range  $3400\text{--}3200\text{ cm}^{-1}$ , there is a new broad peak occurs in the CMC-thiourea complex. This broad peak indicates the existence of OH group in CMC molecules. To strengthen the assumption, it is also clearly shown in the spectra the strong peaks at  $1700\text{--}1670\text{ cm}^{-1}$  which indicates there is carboxylic acid group occurs in the system [20–22].

By comparing the spectra between thiourea dopant and CMC-thiourea complex, obviously the existence of strong peaks at  $1100\text{--}1000\text{ cm}^{-1}$  which was claimed as C-O-C interaction in the system [23]. Thus, it is proven that there were interactions occur between thiourea dopant and CMC molecules in order to obtain the CMC-thiourea system as polymer electrolytes. In the sample, the interaction was detected at these functional groups and can be represented in sample 4. As shown in Fig. 4, there is no interaction between the substituent of thiourea compounds and CMC. It is also expected that the interaction occur at carbonyl group ( $\text{C}=\text{O}$ ) of thiourea compound with oxygen ion ( $\text{O}^-$ ) of CMC.

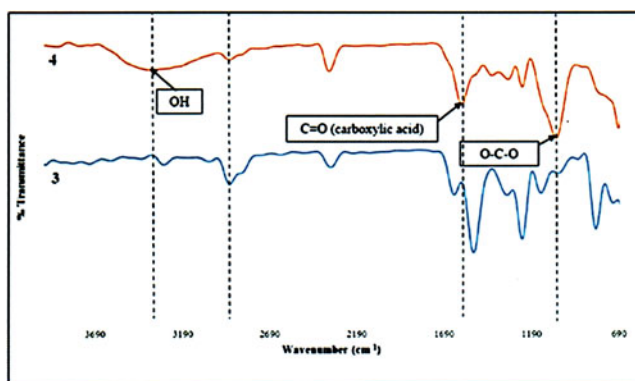
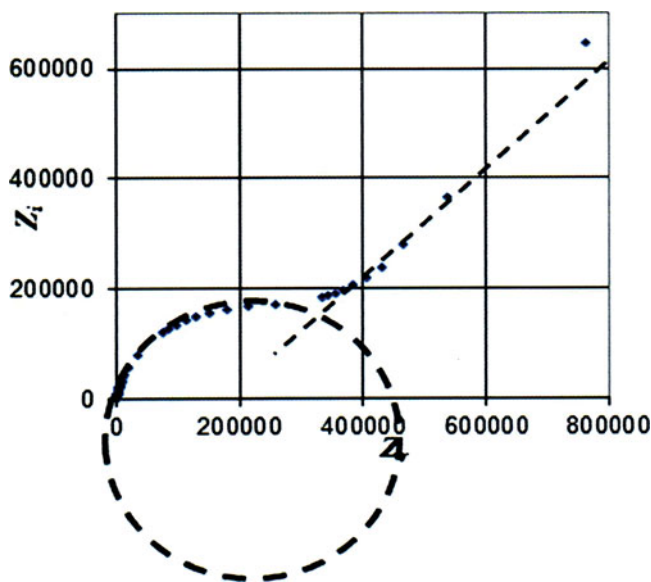


Figure 4. Spectra of CMC-thiourea system (4) in comparison with its dopant (3).



**Figure 5.** The  $R_b$  value obtained from the Cole-Cole Plot and the Cole-Cole Plot of the sample obtained using EIS.

**3.2.2 Conductivity Studies.** The sample of **4** in the form of thin film was cut into four pieces ( $2\text{ cm} \times 2\text{ cm}$ ) and used for analysis by using Electrical Impedance Spectroscopy (EIS). The sample was tested and the sample with the highest ionic conductivity was used for temperature dependence study. From the EIS study conducted using the HIOKI 3532-50 LCR Hi-tester interfaced with a computer, the resultant Cole-Cole plot for each sample was obtained. The Cole-Cole plot is shown in Fig. 5.

From the plots, it can be found typical AC impedance spectra show two well define regions; namely the incomplete semicircle in the high frequency and a spur in the low frequency. The appearance of semicircle can be explained by a parallel combination of resistor and capacitor. The resistor is referred to the migration of ions occur through the free volume of polymer matrix and the capacitor is representing the immobile polymer chains, becoming polarized in the alternating field [24]. The high frequency semicircle can be related to the ionic conduction process in the bulk of the polymer electrolytes, the spectra show spurs at low frequency is attributed to the effect of electrode polarization which is characteristic of diffusion process followed by a semi-circle [25]. It can be related to a charge transfer process [26] with  $Z_i$  intercepts in the higher frequency range and this can attributed to the effect of blocking electrodes.

Since the blocking electrolytes have been used in the impedance analysis, the electrolyte/electrode interface could be regarded as a capacitance. When the capacitance was ideal, it should show a vertical spike in the impedance plot. When the capacitance was ideal, it should show a vertical spike in the impedance plot [27]. However, the spike inclined at an angle ( $\theta$ ) less than  $90^\circ$  has been found instead of the vertical spike which may be attributed to the non-homogeneity or roughness of the electrolyte/electrode interface.

From the Cole-Cole plot, the information of the bulk resistant,  $R_b$  can be obtained in order to calculate the conductivity of the films. The bulk resistance,  $R_b$  can be retrieved from the intercept of high frequency semicircle and the low frequency spike on the  $Z_r$ -axis

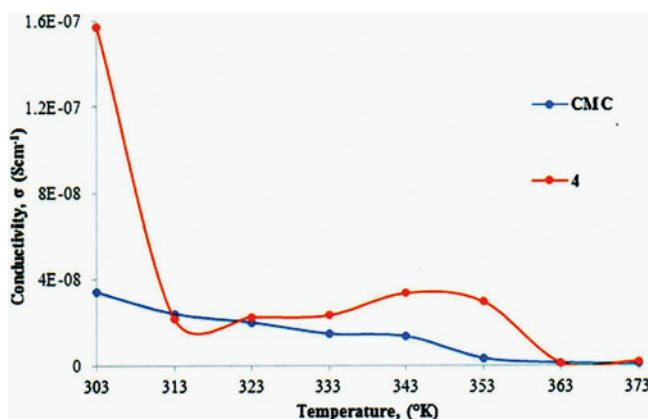


**Figure 6.** The values of conductivity of CMC and the CMC-thiourea (4).

and Equation (1) was used to calculate the conductivity,  $\sigma$  of **4** which is  $1.57 \times 10^{-7} \text{ Scm}^{-1}$  and bulk resistance,  $40734 R_b$  of the sample at room temperature. The conductivity,  $\sigma$  of the CMC-thiourea polymer electrolytes at room temperature is illustrated in Fig. 6.

The conductivity is depicted in Fig. 6 shows that by increasing the temperature it will decrease the conductivity of the sample. The highest conductivity obtained is  $1.57 \times 10^{-7} \text{ Scm}^{-1}$  for **3** at room temperature. Then, as the temperature increases, the conductivity dropped and decreases until zero conductivity at  $373^\circ\text{K}$ . Therefore, it can be concluded that **4** gave higher conductivity value than pure CMC polymer electrolytes which strongly due to the effect of methyl substituent as electron donor in **3**.

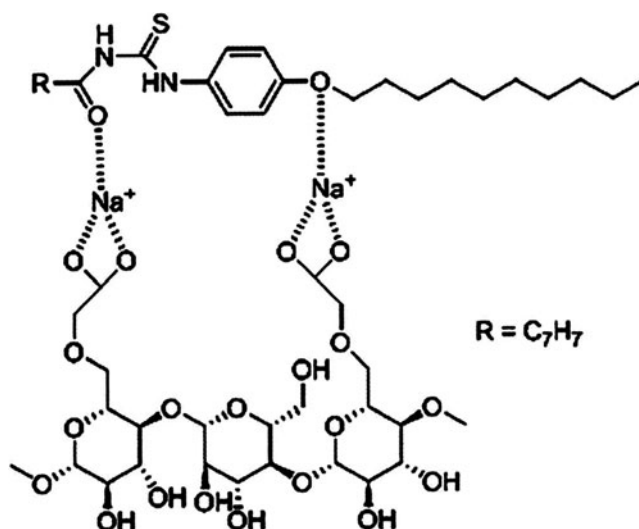


**Figure 7.** The expected molecular structure of the CMC-thiourea complex (4).

**Table 3.** Mulliken effective charges on selected oxygen and sulfur atoms of thiourea and the Na<sup>+</sup> to oxygen distances

| Thiourea derivative | Mulliken charges |        |            | Calculated distances                    |                                       |
|---------------------|------------------|--------|------------|---|---------------------------------------|
|                     | O (C = O amide)  | S      | O (alkoxy) | Distance of Na <sup>+</sup> to O = C, Å | Distance of Na <sup>+</sup> to -O-, Å |
| <b>3</b>            | -0.540[2]        | -0.277 | -0.530[4]  | 2.2393                                  | 2.3137                                |

### 3.3 Theoretical Studies

The dopant, synthesized alkoxy thiourea (**3**) and CMC-thiourea system as polymer electrolyte (**4**) were optimized to the minimum potential energy using Gaussian 09 quantum mechanical software package at the theoretical level of DFT (B3LYP)/6-31G (d,p). From this computational study, we believed that the methyl substituent of thiourea affects the conductivity and thermodynamic properties of the complexes.

In order to predict the molecular structure of the complex between thiourea and CMC, the Mulliken charges values are measured. The Mulliken charges values on the selected atoms of thiourea derivatives are listed in Table 3. Analysis shows that all the charges on oxygen atom of C = O amide was about two times higher than of sulphur atom of thiourea. Slightly the same values of charges were also observed for oxygen atoms of alkoxy. For methylbenzene thiourea derivative (**3**) the charge on oxygen of amide is -0.540 compared to only -0.277 for the sulphur atom. The value of -0.530 is also observed on the oxygen of alkoxy. Due to the higher negative value of charges on oxygen atoms, we believed that the complexes were formed between the COO<sup>-</sup> Na<sup>+</sup> of CMC and the oxygen of amide as a 'head' and another COO<sup>-</sup> Na<sup>+</sup> of CMC to the oxygen alkoxy as a 'tail'. The predicted molecular structure of CMC-thiourea complex is shown in Fig. 7.

An attempt also has been made to optimize the complex formed between thiourea and CMC using the binding site of COO<sup>-</sup> Na<sup>+</sup> to the S (= C) and another end of COO<sup>-</sup> Na<sup>+</sup> to the alkoxy oxygen but the result obtained was unsuccessful. The optimization at the theoretical level of B3LYP/6-31G (d,p) ended with repulsion of the two groups (CMC and thiourea) where the distance between the Na<sup>+</sup> to sulphur is 2.75 Å which is greater than 2.40 Å [28].

However, the optimization of the four complexes using the oxygen carbonyl of amide bonded to Na<sup>+</sup> (COO<sup>-</sup>) resulted with a significant interaction where the distance between the two bonding are in the range of 2.23 to 2.26 Å which is in a good agreement with Yan *et al.*, results [28]. It can be concluded that the complex between **3** was formed by the existence of Coulombic interaction between the Na<sup>+</sup> ion to the carbonyl oxygen of amide at one end and to the alkoxy oxygen on the other hand.

**Table 4.** Total energy, HOMO & LUMO molecular orbital energies, energy band gap, and dipole moment of thiourea derivatives

| Thiourea derivative | SCF energy, au | HOMO, au | LUMO, au | EBG, eV | Dipole moment, D |
|---------------------|----------------|----------|----------|---------|------------------|
| <b>3</b>            | -1631.39160322 | -0.19831 | -0.06516 | 3.62    | 4.5715           |

**Table 5.** Total energy, HOMO & LUMO molecular orbital energies, energy band gap and dipole moment of the complexes formed between thiourea derivatives and CMC.

| Complexes | SCF energy, au | HOMO, au | LUMO, au | EBG,<br>eV | Dipole moment, D |
|-----------|----------------|----------|----------|------------|------------------|
| <b>4</b>  | −4398.02493758 | −0.22344 | −0.09360 | 3.53       | 5.9319           |

*3.3.1 The Prediction of Conductivities.* Table 4 and 5 list the energy band gap (HOMO/LUMO) for thiourea derivative (**3**) and the complexes formed with CMC (**4**) evaluated at 0°K. It can be observed that there were significant changes occurred to the energy band gaps of thiourea during the complexation with CMC. It was clearly seen that there were some reduction to the energy band gap of methylbenzene which is from 3.62 to 3.53 eV. It is believed that this change might affect very much on the conductivity properties of **3** due to the presence of methyl group in the molecular framework.

Meanwhile, in order to determine the relation between the substituents of thiourea (**3**) with the conductivity, the study of  $\text{Ln } \chi^2$  for the first and the second benzene rings in the thiourea derivative evaluated at the theoretical level of B3LYP/6-31G (d,p). As described in the literature [29], these squared of effective charge,  $\chi^2$ , can be used also in the prediction of infrared intensities. In this study the natural logarithm of  $\chi^2$  were employed as a measure of the degree of delocalisation among the benzene rings of the thiourea derivatives. As a standard, the value of the total  $\text{Ln } \chi^2$  for the benzene ring evaluated at the same theoretical level is -31. When there is a substituent existed in the ring, these values should increase to a certain number which represent how far the electron delocalisation deviates from the aromaticity of the benzene ring. It is to our surprise to see that the ranking of these values (total of  $\text{Ln } \chi^2$ ), especially the first ring, exactly were in the same order as experimental results of conductivities, Table 6 and 7 list all the values of  $\text{Ln } \chi^2$  for the first and the second benzene rings in the thiourea derivative of **3** evaluated at the theoretical level of B3LYP/6-31G (d,p).

Based on these theoretical findings, we believed that the conductivities are dependent very much on the delocalization of the first benzene ring of the thiourea derivatives combined with stabilization energies of the complexes with CMC. The stabilization energy is correlated very much to the thermodynamic properties and also to the electrostatic interaction of  $\text{Na}^+$  ion to the carbonyl oxygen of amide group.

### *3.3.2 The Effect of Methyl Substituent on the Stabilization Energy of the Complexes.*

Besides conductivity, the substituents of the thiourea (**3**) also affected the stabilization energy of the complex (**4**). The total electronic energies of the complexes together with the value of the two substituents (thiourea and CMC) are listed in Table 8. Stabilization energies were evaluated by taking the differences between the SCF values of complexes to their two components in question, thiourea and CMC.

As an example, the stabilization energy of **3** was calculated by taking −4398.02493758 au. and then subtracted by the total values of −2766.58227671 au. (CMC) and −1631.38586838 au. (thiourea). The difference of  $5.6792 \times 10^{-2}$  au. was then converted to 149.11 kJ/mol by multiplying with the factor of 2625.50. Results show that methyl substituent formed a stable complexes with CMC with the value of −153.8 kJ/mol. This result is not very far from the reported values of −112 kJ/mol on the complexes formed between

**Table 6.** Mulliken effective charges ( $\chi$ ) and squared effective charges ( $\text{Ln } \chi^2$ ) of all carbon atoms in **the first** benzene ring of the thiourea derivative

| Mulliken charges    |        |                      |        |                      |        |                      |        |                      |        |                      |                              |        |             |
|---------------------|--------|----------------------|--------|----------------------|--------|----------------------|--------|----------------------|--------|----------------------|------------------------------|--------|-------------|
| C1                  |        | C2                   |        | C3                   |        | C4                   |        | C5                   |        | C6                   |                              |        |             |
| Thiourea derivative | $\chi$ | $-\text{Ln } \chi^2$ | $\chi$ | $-\text{Ln } \chi^2$ | $\chi$ | $-\text{Ln } \chi^2$ | $\chi$ | $-\text{Ln } \chi^2$ | $\chi$ | $-\text{Ln } \chi^2$ | Total $[-\text{Ln } \chi^2]$ |        |             |
| <b>3</b>            | -0.133 | 4.0348               | -0.126 | 4.1429               | -0.120 | 4.2405               | +0.042 | 6.3402               | -0.088 | 4.8608               | -0.126                       | 4.1429 | 27.7621 [2] |

**Table 7.** Mulliken effective charges ( $\chi$ ) and squared effective charges ( $\text{Ln } \chi^2$ ) of all carbon atoms in **the second** benzene ring of the thiourea derivative, a) before and b) during the formation of the complex with CMC

| Mulliken charges |        |                      |        |                      |        |                      |        |                      |        |                      |                              |        |             |
|------------------|--------|----------------------|--------|----------------------|--------|----------------------|--------|----------------------|--------|----------------------|------------------------------|--------|-------------|
| C7               |        | C8                   |        | C9                   |        | C10                  |        | C11                  |        | C12                  |                              |        |             |
| Thiourea         | $\chi$ | $-\text{Ln } \chi^2$ | $\chi$ | $-\text{Ln } \chi^2$ | $\chi$ | $-\text{Ln } \chi^2$ | $\chi$ | $-\text{Ln } \chi^2$ | $\chi$ | $-\text{Ln } \chi^2$ | Total $[-\text{Ln } \chi^2]$ |        |             |
| <b>3</b>         | +0.316 | 2.3040               | -0.074 | 5.2074               | -0.143 | 3.8898               | +0.363 | 2.0267               | -0.137 | 3.9755               | -0.149                       | 3.8076 | 21.2110 [2] |

**Table 8.** SCF energy of the complexes, CMC and thiourea derivatives during complexation and stabilisation energy of the complexes

| Complexes | SCF energy, au<br>(complex) | SCF energy, au<br>(CMC) | SCF energy, au<br>(thiourea) | Stabilization<br>energy, kJ/mol |
|-----------|-----------------------------|-------------------------|------------------------------|---------------------------------|
| <b>4</b>  | −4398.02493758              | −2766.58227671          | −1631.38586838               | −149.1087[4]                    |

Na<sup>+</sup> and O-cresol [28]. Our results cannot be compared directly with their findings due to the different number of Na<sup>+</sup> . . . O linkages and different type of molecules involved.

This order of stabilization energies can be used to explain why the methylbenzene complexes with CMC easily collapse at evaluated temperatures of higher than 33°C.

#### 4. Conclusion

Alkoxy substituted thiourea featuring methyl substituent has been successfully synthesised and characterised via typical spectroscopic and analytical techniques. In turn, CMC-thiourea polymer electrolyte system has been successfully prepared via solution casting technique. Through computational chemistry study via Gaussian 09 Quantum Mechanical Software Package, the complex interaction was proven between the COO<sup>−</sup> Na<sup>+</sup> of CMC and the oxygen of amide and another COO<sup>−</sup>Na<sup>+</sup> of CMC to the oxygen at alkoxy. Besides, the substituent of the thiourea also affected the conductivity of the complex due to its effective charges ( $\chi^2$ ) of the aromatic portion. Thus, the conductivity analysis carried out was in the agreement of the computational analysis. Thus, conclusion can be made that the synthesized thiourea compound in this work is potentially can be used as conducting polymer.

#### Acknowledgments

Special acknowledgment is dedicated to Ministry of Higher Education, Malaysia (MOHE) for the funding of this research (FRGS 59253), MyBrain 15 for postgraduate scholarship, Advanced Materials Research Group, School of Fundamental Science, Institute of Marine Biotechnology (IMB) and Institute of Oceanography and Environment (INOS), Universiti Malaysia Terengganu (UMT) for NMR and SEM analysis respectively.

#### References

- [1] Zheng, W., Yates, S. R., Papiernik, S. K., & Guo, M. (2004). *Environ. Sci. Technol.*, 38 (24), 6855.
- [2] Saeed, S., Rashid, N., Jones, P. G., Ali, M., & Hussain, R. (2010). *European Journal of Medicinal Chemistry*, 45, 132.
- [3] Shao, J., Yu, M., Lin, H., & Lin, H. (2008). *Spectrochimica Acta Part A*, 70, 1217.
- [4] Jose, D. A., Singh, A., Das, A. & Ganguly, B. (2007). *Tetrahedron Lett.*, 48, 3695.
- [5] Kumari, R. G., Ramakrishnan V., Carolin M. L., Kumar, J., Sarua, A., & Kuball, M. (2009). *Spectrochimica Acta Part A*, 73, 263.
- [6] Adli, H. K., Khairul, W. M., & Salleh, H. (2012). *Int. J. Electrochem.*, 7, 499.
- [7] Shen, C. B., Wang, S. G., Yang, H. Y., Long, K., & Wang, F. H. (2006). *Corrosion Science*, 48, 1655.
- [8] Yang, D., Chen, Y.-C., & Zhu, N.-Y. (2004). *Org. Lett.*, 6(10), 1577.



- [9] Zhao, P., Wang, P., Zhang, Z., Fang, C., Wang, Y., Zhai, Y., & Liu, D. (2009). *Solid State Comms.*, 149, 928.
- [10] Wang, N., Zhang, X., Liu, H., & He, B. (2009). *Carbohydrate Polymers*, 76, 482.
- [11] Barbucci, R., & Goyal, P. S. (2005). *Journal of Non-Crystalline Solids*, 351, 1573.
- [12] Marci, G., Mele, G., Palmisano, L., Pulito, P., & Sannino, A. (2006). *Green Chemistry*, 8, 439.
- [13] Rozali, M. L. H., Samsudin, A. S., & Isa, M. I. N. (2012). *International Journal of Applied Science and Technology*, 2(4), 113.
- [14] Chandrasekaran, S., Ezhakudiyar, R., Jeevarathinam, A. S., Narayanasastri, S., & Baran, A. (2012). *Journal of materials Chemistry*, 22, 18975.
- [15] Lixin, W., Guowen, L., & Yingqiu, L. (1992). *Chemical Research in Chinese Universities*, 8, 428.
- [16] Williams, D. H., & Fleming, I. (1995). *Spectroscopic Methods in Inorganic Chemistry*, 5th ed.; McGraw-Hill.
- [17] Pavia, D. L., Lampman, G. M., & Kriz, G. S. (2001). *Introduction to Spectroscopy*, Third ed. pp 358–379. Thomson learning, Inc.
- [18] Khairul, W. M., Yusof, M. F., Rahamathullah, R., Daud, A. I., Jasman, S. M., Hasan, M. F. A., Salleh, H., Adli, H. K., & Tay, M. G. (2013). *Int. J. Electrochem. Sci.*, 8, 8175.
- [19] Yang, W., Weiqun, Z., & Zhang, Z. (2007). *J. Mol. Struct.*, 828, 46.
- [20] Pushpamalar, V., Langford, S. J., Ahmad, M., & Lim, Y. Y. (2006). *Carbohydr. Polym.*, 64, 312.
- [21] Wang, N., Zhang, X., Liu, H., & He, B. (2009). *Carbohydr. Polym.*, 76, 482.
- [22] Ho, C.-H., Shieh, C.-Y., Tseng, C. L., Chen, Y.-K., & Lin, J.-L. (2008). *J. Catal*, 261, 150.
- [23] Nik Aziz, N. A., Idris, N. K., & Isa, M. I. N. (2010). *Int. J. of Polym. Anal. Charact.*, 15, 319.
- [24] Ramya, C. S., Selvasekarapandian, S., Hirankumar, G., Savitha, T., & Angelo, P. C. (2008). *Journal of Non-Crystalline Solids*, 354, 1494.
- [25] Hema, M., Selvasekarapandian, S., Sakunthala, A., Arunkumar, D., & Nithya, H. (2008). *Physica B*, 403, 2740.
- [26] Appetecchi, G. B., Croce, F., & Scrosati, B. (1995). *Electrochimica Acta*, 40, 991.
- [27] Selvasekarapandian, S., Hema, M., Hirankumar, G., Sakunthala, A., Arunkumar, D., & Nithya, H. (2010). *Journal of Spectrochimica Acta Part A*, 75, 474.
- [28] Yan, Y.-G., Shi, W.-J., Feng, G.-R., Ren, F.-D., & Wang, Y. (2012). *Computational and Theoretical Chemistry*, 996, 91.
- [29] Person, W. B., & KuBulat, K. (1990). *Journal of Molecular Structure*, 224, 225.